Nuclear Engineering and Technology 58 (2026) 103907

Contents lists available at ScienceDirect

Nuclear Engineering and Technology

journal homepage: www.elsevier.com/locate/net

Original Article

The study of characteristics of flat panel detectors without semiconductor conversion layers for therapeutic high-energy X-ray radiation

Dong Ho Lee [a,b,e,1], Sangmin Lee [a,1], Hyounggun Lee [c], Kyunghoon Yoon [d], Kang Heo [d], Yeong Jun Han [d], Dooho Kim [d], Jeyong Jeon [d], Hyeon Jae Yu [d], Dong Wook Kim [a,*], Jin Sung Kim [a,**]

[a] Department of Radiation Oncology, Yonsei Cancer Center, Heavy Ion Therapy Research Institute, Yonsei University College of Medicine, Seoul, Republic of Korea
[b] Dept. of Integrative Medicine Major in Digital Healthcare, Yonsei University College of Medicine, Republic of Korea
[c] Medical Accelerator Research Team, Korea Institute of Radiological and Medical Sciences, Seoul, 01812, Republic of Korea
[d] Vieworks, 41-3, Burim-ro 170, Dongan-gu, Anyang-si, Gueonggi-do, Republic of Korea
[e] Medical Physics and Biomedical Engineering Lab (MPBEL), Yonsei University College of Medicine, Seoul, Republic of Korea

ARTICLE INFO

Keywords:
TFT
Detector
Radiation
Therapy
Dose
X-ray

ABSTRACT

We evaluated a novel 2-D flat-panel detector (FPD) adapting it for megavoltage (MV) therapeutic imaging and radiation QA. The prototype uses a thick dielectric layer to create a semi-transmissive structure, changing and eliminating structure conventional semiconductor conversion layers. Performance was tested on a Harmony Pro LINAC (Elekta, Sweden) with a 20 × 20 cm^2 field at an SSD of 100 cm. Datasets were acquired at 50–300 MU for 6, 10, and 15 MV beams. Linearity with MU was excellent ($R^2 = 0.99$). Reproducibility and repeatability showed coefficients of variation of 1–2 %. In energy dependency, the 6/10 MV response ratio remained near 80 %, rising to 84 % at 300 MU, while the 6/15 MV ratio was 70.8 % at 50 MU and stabilized at 75–80 % thereafter, with $R^2 > 0.99$ for all energies. Spatial resolution satisfied AAPM TG-142 tolerances. The detector demonstrates performance characteristics comparable to those of conventional electronic portal imaging device (EPID), exhibiting robust durability in high-energy irradiation and excellent portability enabled by its compact design.

1. Introduction

In recent years, the demand for advanced detectors in radiation therapy has significantly increased, driven by the need for accurate and safe treatment delivery. Flat-panel detectors (FPDs) have become essential components in both diagnostic X-ray imaging and high-energy therapeutic applications due to their superior energy resolution and sensitivity, substantially enhancing image quality and treatment precision [1–4].

Beyond conventional patient imaging, two-dimensional (2D) measurement techniques now play a critical role in quality assurance (QA), ensuring precise dose delivery and improving overall treatment effectiveness [5,6]. The commonly employed 2D QA methods include semiconductor-based FPDs and radiochromic films [6]. Radiochromic films offer exceptional spatial resolution, water-equivalent properties, and a thin profile (278 μm), making them suitable for accurate 2D dose measurements [7]. However, their requirement for extensive development time (approximately 8 h) before readout precludes real-time feedback, necessitating batch-specific dose calibration. Additionally, their single-use nature elevates long-term operational costs. Electronic portal imaging devices (EPIDs), consisting of semiconductor materials, are frequently used for obtaining high-resolution images; nonetheless, their effectiveness can be compromised by intrinsic semiconductor properties, pixel size limitations, and sensitivity degradation due to radiation-induced aging. Furthermore, substantial installation and maintenance costs pose significant clinical challenges [8].

Semiconductor-based 2D detectors, utilizing materials such as amorphous selenium, directly convert radiation into electrical signals through electron-hole pair generation [9]. This direct detection approach typically provides superior resolution compared to indirect methods, where scintillator materials convert radiation to visible light first. Despite these advantages, semiconductor-based detectors can

* Corresponding author.
** Corresponding author.
E-mail addresses: kdw1026@yuhs.ac (D.W. Kim), JINSUNG@yuhs.ac (J.S. Kim).
[1] These authors are equally contributed this article.

https://doi.org/10.1016/j.net.2025.103907
Received 13 May 2025; Received in revised form 13 August 2025; Accepted 3 September 2025
Available online 10 September 2025
1738-5733/© 2026 Korean Nuclear Society, Published by Elsevier Korea LLC. All rights are reserved, including those for text and data mining, AI training, and similar technologies. This is an open access article under the CC BY-NC-ND license (http://creativecommons.org/licenses/by-nc-nd/4.0/).

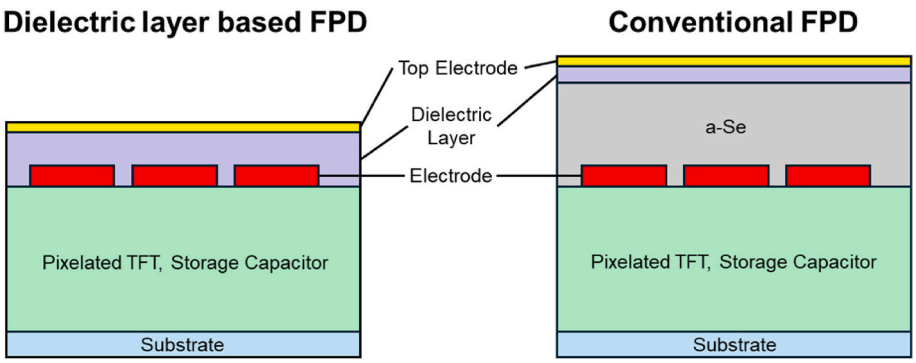

Fig. 1. Simplified illustrations of a dielectric layer based FPD and conventional FPD.

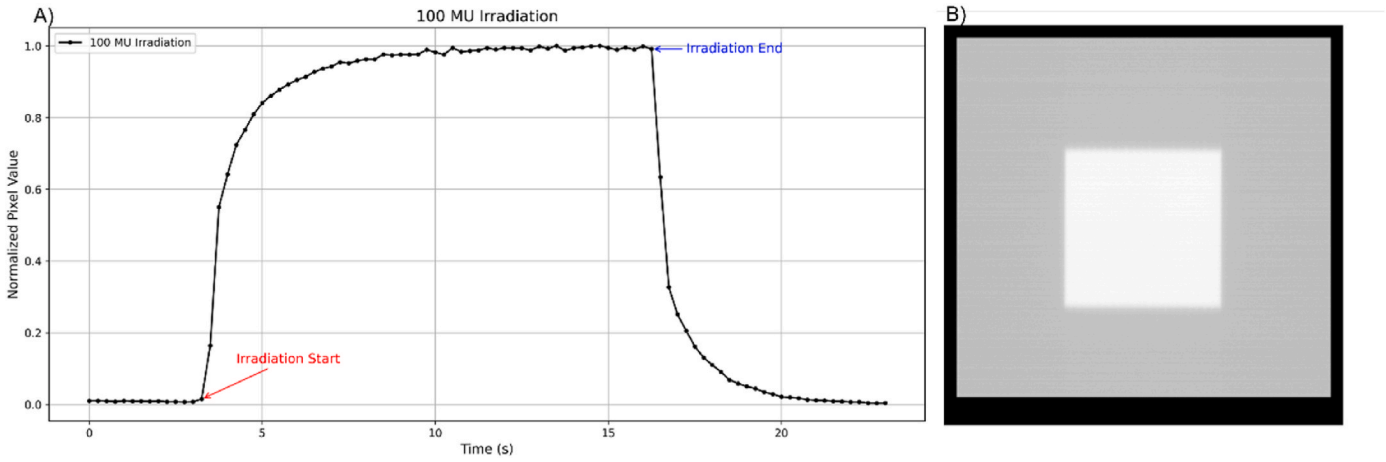

Fig. 2. A) The response of the detector during a 100 MU irradiation, recorded at 4 fps. B) The 2D image of 100 MU irradiation with a 20 × 20 cm^2 field.

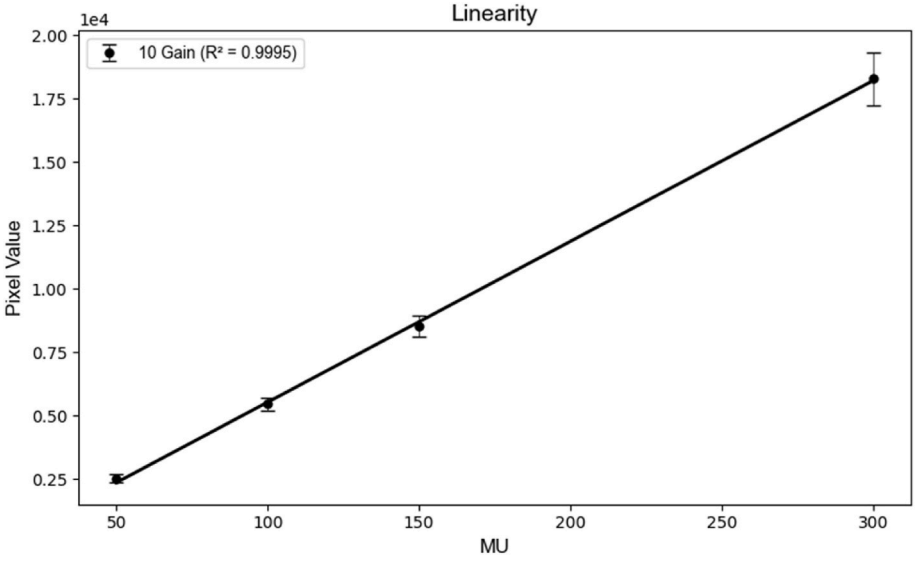

Fig. 3. Detector response measured at 50–300 MU. Black line indicated the linear regression fit.

experience performance degradation over time and possess inherent constraints regarding spatial resolution and response speed.

Previous studies have demonstrated that commercially available semiconductor-based FPDs perform effectively in diagnostic and portal imaging systems utilizing kilovoltage (kV) photon beams [10,11]. However, further investigation is required to confirm their performance under megavoltage (MV) therapeutic radiation conditions.

Addressing these needs, a novel dielectric-based FPD structure design is developed explicitly for high-energy and high-intensity radiation environments. By removing the semiconductor charge-generating layer and integrating a thicker dielectric layer, this innovative design establishes ionization paths under intense radiation exposures, thereby reducing charge trapping and enhancing image quality [12].

Considering the recognized limitations of semiconductor-based

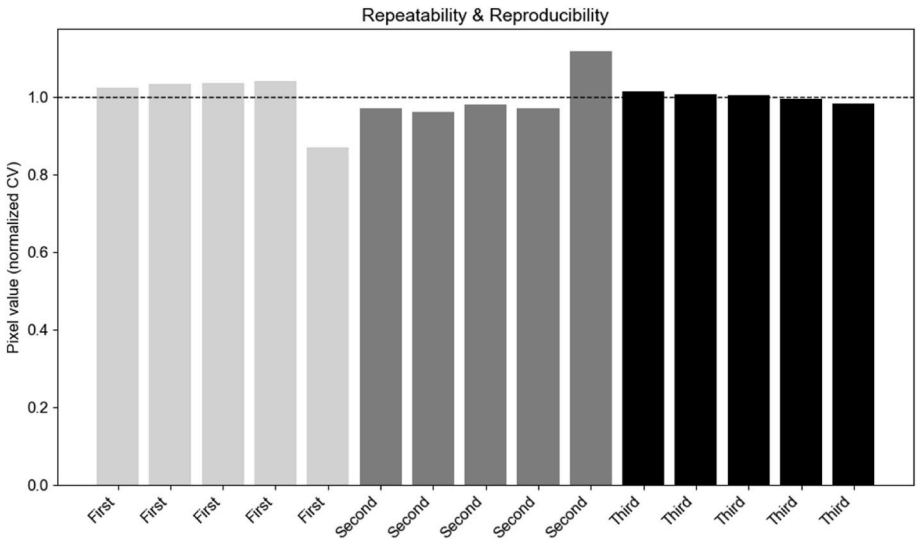

Fig. 4. A comparative analysis was performed on the detector responses obtained from consecutive 100 MU beam acquisitions conducted on different measurement dates.

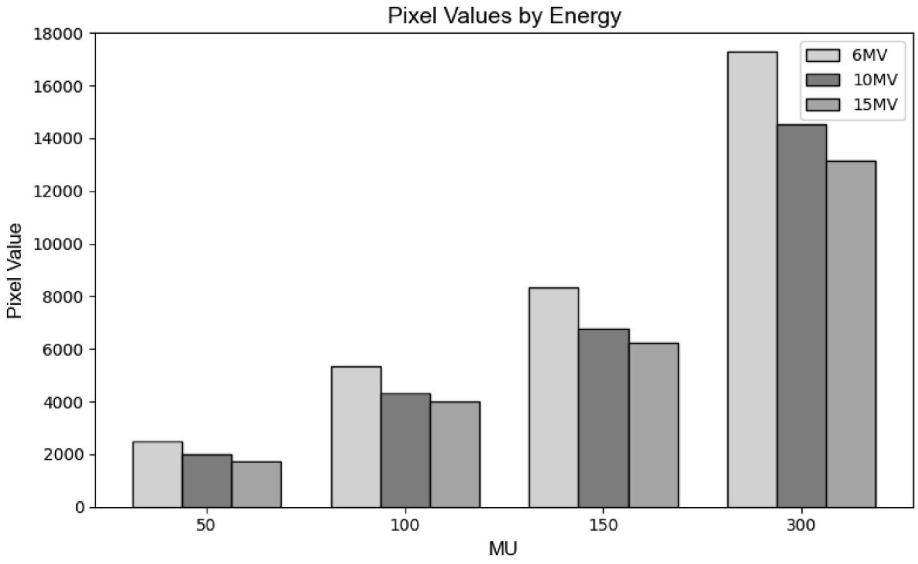

Fig. 5. Measurements were conducted at MU settings of 50, 100, 150, and 300 across photon beam energies of 6, 10, and 15 MV. Light gray bars represent 6 MV, dark gray bars represent 10 MV, and gray bars represent 15 MV.

Table 1
These values represent the spatial resolution and contrast of images measured with high-energy photon beams. The reference values were obtained from images acquired using QC-3 phantom on the Electronic Portal Imaging Device (EPID) of the Harmony Pro system.

Image Quality Parameters	Measured	Reference
Spatial Resolution *(50 % MTF)*	0.47 lp/mm	0.50 lp/mm
Contrast	17.6 %	18.2 %

FPDs, including long-term degradation and restricted resolution and response speed, characterizing this new dielectric-based FPD for high-energy radiation applications is essential. Consequently, this study systematically evaluates the performance and clinical applicability of dielectric-based FPDs for high-energy therapeutic photon beams. Key performance parameters, including linearity, reproducibility, repeatability, energy dependency, and resolution, are comprehensively analyzed to ensure the detector's consistency, accuracy, and reliability.

2. Materials and methods

2.1. Experimental conditions

2.1.1. Dielectric based FPD

In contrast to conventional FPDs that utilize amorphous selenium as the primary charge-generating medium, the detector used in this study replaces this layer with a Kapton polyimide dielectric material (Fig. 1). In typical semiconductor-based FPD structures, the dielectric layer serves to prevent charge accumulation at the top electrode. However, in this newly developed dielectric-based FPD, a substantially thicker (38 μm) dielectric layer is used. The dielectric layer shows radiation induced conductivity [13]. Consequently, electrons generated within the dielectric layer can be collected by the electrode and the TFT layer under high-intensity radiation. As a result, although the overall charge-generation efficiency is relatively low, the detector demonstrates a more stable response under high-intensity and high-dose irradiation conditions, thereby enhancing its suitability for therapeutic applications

Table 2
The performance of commercial detectors, including EPID, iQM, MatriXX, and MapCHECK, on the Linac was compared with that of the newly developed detector by Vieworks.

Evaluation Parameters	Vieworks	iQM	MatriXX	MapCHECK	EPID *(CCD Based)*
Linearity (%)	0.99	About 1	0.99	0.99	0.98
Reproducibility (%)	0.83–2.12	0.47	0.75–1.08	1	0.8
Repeatability (%)	0.84–1.05	0.14	0.8	Under 1	Within 2
Spatial Resolution (lp/mm)	0.47	0.28–0.33	0.55	–	0.41

[12].

2.1.2. LINAC irradiation

To evaluate the performance of the FPD, a linear accelerator (LINAC) (Harmony Pro, Elekta, Sweden) was used. This LINAC undergoes regular quality assurance (QA) procedures, ensuring that at 6, 10, and 15 MV photon energies, an output of 100 monitor units (MU) corresponds to 100 cGy delivered at the depth of maximum dose [14–16]. For this study, the reference condition was set to 6 MV, a 20 × 20 cm^2 field size, a source-to-surface distance (SSD) of 100 cm, and 100 MU. Variations in these parameters were then introduced to comprehensively assess the detector's characteristics.

2.1.3. Signal processing

In this study, when the beam was delivered using the field size of 20 × 20 cm^2, the detector's response was obtained by defining a 16 × 16 cm^2 region of interest (ROI) at the center of the field and calculating the mean pixel value within that area. Furthermore, during beam irradiation, images acquired at 4 frames per second were used to calculate the mean pixel value of each frame, and these values were then merged to derive the overall average response (Fig. 2).

2.2. Measurement items for the detector characteristics

2.2.1. Linearity

To assess the detector's response at various dose levels, the several MU settings were used including 50, 100, 150, and 300 MU. Linearity was evaluated by plotting the relationship between the measured responses and the corresponding MU settings, and the coefficient of determination (R^2) was calculated via linear regression analysis to confirm the detector's linear response. The formula for the coefficient of determination (R^2) is as follows:

$$R^2 = 1 - \frac{\sum (y_i - \hat{y}_i)^2}{\sum (y_i - \bar{y})^2} \quad (1)$$

, where y_i are the actual values, $\hat{y}_i$ are the predicted values from the regression model, $\bar{y}$ is the mean of the actual values.

2.2.2. Repeatability

The measurements were repeated 5 times to assess the repeatability of the detector. The MU were also varied among four levels (50, 100, 150, and 300 MU), with each MU value measured 5 times continuously without changing the experiment setup. Then the responses were statistically analyzed to calculate the average and standard deviation.

2.2.3. Reproducibility

Measurements were conducted on different days over a period of several months, maintaining identical experimental setup and beam conditions. The mean and standard deviation were calculated through statistical analysis, and the coefficient of variation was derived from these values to evaluate reproducibility. A lower coefficient of variation indicates higher reproducibility. The percentage difference is calculated as follows:

$$Coefficient\ of\ Variation = \frac{Response_{averaged} - Response_{each\ \ day}}{Response_{averaged}} \times 100 \quad (2)$$

, where the $Response_{averaged}$ represents the average value of response data obtained under consistent experimental conditions.

2.2.4. Energy dependency

LINAC uses various photon energies to deliver prescribed dose to tumor target depending on its location and depth. Therefore, to use FPD for the beam QA procedure, the energy dependency of FPD should be measured. The energy dependency was measured by varying photon beam energies (6, 10, and 15 MV). To assess the detector's response across different photon energies, MU settings of 50, 100, 150, and 300 were utilized.

2.2.5. Resolution

To analyze the resolution, the QC-3 phantom (Standard Imaging, United States) was utilized, and the analysis was performed using the same methods applied in clinical LINAC systems for quality assurance with phantoms suitable for evaluation at megavoltage levels. This setup allowed for the assessment of spatial resolution and contrast corresponding to 50 % modulation transfer function (MTF). These values are compared with the clinical tolerance criteria recommended by AAPM Task Group 142 [15].

Linearity, reproducibility, repeatability, and energy dependency were evaluated based on the average pixel values within designated regions of interest (ROIs). In contrast, resolution analysis was performed using an accumulated dose image acquired during radiation exposure, thereby providing a different perspective on the detector's performance. Through this comprehensive analytical approach, the performance indicators of the FPD were systematically evaluated, and its characteristics as a radiation detector were thoroughly characterized.

3. Results

3.1. Linearity

As a result of measuring the radiation intensity from low MU to high MU in steps at 6 MV energy, the pixel value of the detector showed a linear relationship to MUs. The linear regression analysis yielded a correlation coefficient (R^2) of 0.99, indicating an excellent degree of linearity (Fig. 3). Residual analysis of the detector's output signals at MU settings of 50, 100, 150, and 300 revealed that at 100 MU, the mean pixel value was 5456 representing a 1.4 % deviation from the value predicted by the linear regression model. Furthermore, the residuals for all data points remained within 2 % of their predicted values. These results provide further evidence that the detector exhibits a consistent response across a wide range of radiation energy levels.

3.2. Repeatability & reproducibility

Reproducibility was evaluated by acquiring the detector signal at 100 MU under identical photon-beam parameters. The coefficient of variation (CV) of pixel values within a centrally placed 20 × 20 cm^2 ROI remained below 2 %, demonstrating minimal inter-session variability and excellent stability under fixed exposure conditions.

Repeatability was assessed by performing five consecutive acquisitions at 100 MU, yielding coefficients of variation of 0.86 %, 0.84 %, and 1.05 %, respectively, thereby demonstrating high intra-session

consistency and negligible variation between successive measurements (Fig. 4).

Taken together with the detector's demonstrated linear response across varying MU settings, these results confirmed that, even when beam output energy change, the detector provided superior reproducibility and repeatability under identical exposure conditions (Fig. 3).

3.3. Energy dependency

Measurements were performed with 6, 10, and 15 MV photon beams, and the detector output exhibited a dependence on beam energy. Furthermore, evaluation of linearity across varying MUs showed slopes of 59.51, 50.52, and 45.61 pixels/MU for 6, 10, and 15 MV, respectively, with all coefficients of determination (R^2) exceeding 0.99.

Energy dependency was evaluated by comparing responses at identical MU settings relative to 6 MV. The 6 MV-10MV response ratio remained near 80 % across 50–150 MU and rose modestly to 84 % at 300 MU. For 15 MV, ratio was lowest (70.8 %) at 50 MU before stabilizing around 75 % at higher MUs. Although both higher energies showed a slight upward trend in relative response with increasing MU, their ratios remained generally constant throughout the tested range (Fig. 5).

3.4. Resolution

When spatial resolution and contrast were evaluated using the QC-3 phantom acquired at high energy levels, the results were compared against the acceptance test procedure (ATP) values recommended by AAPM Task Group 142. The measured contrast was 17.6 %, which was 0.6 % lower than the previously reported value of 18.2 %. However, the spatial resolution was measured at 0.47 lp/mm, indicating improved performance compared to the ATP benchmark of 0.50 lp/mm.

4. Discussion

In this study, the FPD incorporating a dielectric sensitive layer was characterized under MV therapeutic photon beams with respect to linearity, repeatability, reproducibility, energy dependence, and spatial resolution as shown in Table 1. The detector met performance benchmarks suitable for 2D dosimetry and imaging, indicating its potential application in patient-specific quality assurance and routine LINAC QA. As shown in Table 2, the detector exhibits comparable performance to other commercial LINAC QA detectors [17–25]. Especially, the dielectric layer of this FPD is fabricated from a transparent material. This allows for the simple detachment of opaque components such as the TFT panel, enabling the transmission of the LINAC's light field while the FPD remains attached to the LINAC head. This feature facilitates mechanical quality assurance (QA) procedures without the need to detach the entire FPD from LINACs. Furthermore, it enables real-time acquisition of 2D beam profiles during patient treatment beam delivery. Unlike Electronic Portal Imaging Devices (EPIDs) that measure the transmitted beam after passing through the patient, this approach allows for the measurement of the incident beam, potentially leading to more accurate dose calculations.

In addition, this study investigated the phenomenon of lagging during the imaging process of the radiation detector. Lagging, characterized by the persistence of afterimages in the detector output, was observed, with pixel values diminishing within a few seconds. This effect is particularly critical in high-energy radiation therapy, necessitating further investigation in future studies to reduce lagging time for more accurate response. Moreover, implementing a complete pixel reset during calibration, rather than relying on uniform output images, could facilitate a more thorough examination of the reliability and stability of the detector's output.

This study also highlights the imperative for further research on QA in radiation therapy. The QA is essential for monitoring and evaluating the performance and safety of medical equipment throughout the treatment process. The findings of this study demonstrate the potential of FPDs, confirming their applicability for the QA and high-energy treatments. Prior to evaluating the detector's performance, an irradiation 5000 MU at 6 MV was conducted both for hardness testing and to serve as a warm-up procedure. The data collected under these conditions demonstrate the detector's robustness in handling high radiation intensities, confirming its stability and reliability in high-dose scenarios. In future work, Investigating the QA validity of FPDs can significantly enhance the quality and consistency of medical equipment performance across all clinical procedures.

5. Conclusion

The novel dielectric layer based FPD demonstrated robust performance to use in 2D dosimetry and imaging of MV photon beams on a clinical LINAC. Owing to its optically transparent sensitive layer, the device facilitates straightforward setup with light field of LINAC, and seamless integration into both routine machine QA and patient-specific verification workflows. Provided that the residual lagging time (few seconds) is further mitigated through refined readout electronics and post-processing algorithms, the detector will be well positioned to serve as a practical QA instrument in clinical radiotherapy.

CRediT authorship contribution statement

Dong Ho Lee: Writing – original draft, Project administration, Methodology, Investigation, Formal analysis, Data curation, Writing – review & editing, Conceptualization, Validation. **Sangmin Lee:** Writing – review & editing, Validation, Methodology, Formal analysis, Data curation, Conceptualization, Investigation, Project administration, Writing – original draft. **Hyounggun Lee:** Validation, Methodology. **Kyunghoon Yoon:** Software, Resources. **Kang Heo:** Software, Resources. **Yeong Jun Han:** Software, Resources. **Dooho Kim:** Software, Resources. **Jeyong Jeon:** Software, Resources. **Hyeon Jae Yu:** Software, Resources. **Dong Wook Kim:** Writing – review & editing, Supervision. **Jin Sung Kim:** Supervision.

Statement

During the preparation of this manuscript the authors used ChatGPT to improve readability. After using this tool, the authors reviewed and edited the contents as needed and take full responsibility for the content of the publication.

Declaration of interest

The authors acknowledge funding from Vieworks Co., Ltd(Grant No. 2024-31-0540), which may present a potential competing interest. However, the funding source had no role in the conduct of the research or preparation of this article.

Acknowledgements

This work was supported by Vieworks Co., Ltd (Grant No. 2024-31-0540), by a faculty research grant of Yonsei University College of Medicine (6-2021-0234), by Korea Institute for Advancement of Technology (KIAT) grant funded by the Korea Government (P0026103) and by the Nuclear Safety Research Program (RS-2022-KN071210) through the Korea Foundation of Nuclear Safety (KOFONS) using the financial resource granted by the Nuclear Safety and Security Commission (NSSC) of the Republic of Korea.

References

[1] D.A. Jaffray, Image-guided radiotherapy: from current concept to future perspectives, Nat. Rev. Clin. Oncol. 9 (12) (2012) 688–699.

[2] M. Korner, et al., Advances in digital radiography: physical principles and system overview, Radiographics 27 (3) (2007) 675–686.
[3] J.A. Seibert, Flat-panel detectors: how much better are they? Pediatr. Radiol. 36 (2006) 173–181.
[4] L.E. Antonuk, et al., Development of thin-film flat-panel arrays for diagnostic and radiotherapy imaging, in: Medical Imaging VI: Instrumentation, SPIE, 1992.
[5] S. Yaddanapudi, et al., Rapid acceptance testing of modern linac using on-board MV and kV imaging systems, Medical physics 44 (7) (2017) 3393–3406.
[6] B. Hartmann, et al., Investigations of a flat-panel detector for quality assurance measurements in ion beam therapy, Phys. Med. Biol. 57 (1) (2011) 51.
[7] S. Devic, N. Tomic, D. Lewis, Reference radiochromic film dosimetry: review of technical aspects, Phys. Med. 32 (4) (2016) 541–556.
[8] W. Van Elmpt, et al., A literature review of electronic portal imaging for radiotherapy dosimetry, Radiother. Oncol. 88 (3) (2008) 289–309.
[9] L.E. Antonuk, et al., Megavoltage imaging with a large-area, flat-panel, amorphous silicon imager, Int. J. Radiat. Oncol. Biol. Phys. 36 (3) (1996) 661–672.
[10] T. Khalil, et al., Review of flat panel detectors technique for medical imaging quality improvement, in: AIP Conference Proceedings, AIP Publishing, 2020.
[11] P.J. Sellin, Recent advances in compound semiconductor radiation detectors, Nucl. Instrum. Methods Phys. Res. Sect. A Accel. Spectrom. Detect. Assoc. Equip. 513 (1–2) (2003) 332–339.
[12] D.L. Lee, et al., Novel direct conversion imaging detector without selenium or semiconductor conversion layer, in: Medical Imaging 2019: Physics of Medical Imaging, SPIE, 2019.
[13] E.A. Plis, et al., Review of radiation-induced effects in polyimide, Appl. Sci. 9 (10) (2019) 1999.
[14] P.R. Almond, et al., AAPM's TG-51 protocol for clinical reference dosimetry of high-energy photon and electron beams, Medical physics 26 (9) (1999) 1847–1870.
[15] E.E. Klein, et al., Task group 142 report: quality assurance of medical accelerators a, Medical physics 36 (9Part1) (2009) 4197–4212.
[16] Absorbed Dose Determination in External Beam Radiotherapy, INTERNATIONAL ATOMIC ENERGY AGENCY, Vienna, 2024.
[17] O.M. Oderinde, F. du Plessis, Sensitivity of the IQM and MatriXX detectors in megavolt photon beams, Rep. Practical Oncol. Radiother. 24 (5) (2019) 462–471.
[18] D. Hoffman, et al., Characterization and evaluation of an integrated quality monitoring system for online quality assurance of external beam radiation therapy, J. Appl. Clin. Med. Phys. 18 (1) (2017) 40–48.
[19] E.M. McKenzie, et al., Reproducibility in patient-specific IMRT QA, J. Appl. Clin. Med. Phys. 15 (3) (2014) 241–251.
[20] J.G. Li, G. Yan, C. Liu, Comparison of two commercial detector arrays for IMRT quality assurance, J. Appl. Clin. Med. Phys. 10 (2) (2009) 62–74.
[21] S.J. Blake, et al., Characterization of a novel EPID designed for simultaneous imaging and dose verification in radiotherapy, Medical physics 40 (9) (2013) 091902.
[22] A. Van Esch, T. Depuydt, D.P. Huyskens, The use of an aSi-based EPID for routine absolute dosimetric pre-treatment verification of dynamic IMRT fields, Radiother. Oncol. 71 (2) (2004) 223–234.
[23] P.B. Greer, C.C. Popescu, Dosimetric properties of an amorphous silicon electronic portal imaging device for verification of dynamic intensity modulated radiation therapy, Medical physics 30 (7) (2003) 1618–1627.
[24] D. Dudas, et al., The effect of MV image spatial resolution on the patient positioning and patient specific QA, J. Instrum. 16 (12) (2021) T12018.
[25] R.C. Tegtmeier, et al., Performance evaluation of image reconstruction algorithms for a megavoltage computed tomography system on a helical tomotherapy unit, Biomedical Physics & Engineering Express 8 (4) (2022) 047001.